ISSN: 2456-9348
Vol (02) _Issue (04) Impact Factor: 4.520

iJETRM
International Journal of Engineering Technology Research & Management

NUMERICAL ANALYSIS FOR FAILURE OF PRESSURE TUBES IN ADVANCED HEAVY WATER REACTOR (AHWR)

Tikendra Nath Verma*[1]
Prerana Nashine [2]
Moon Banerjee[3]
[*1]Department of Mechanical Engineering, National Institute of Technology Manipur-795004, India
[2] Department of Mechanical Engineering, National Institute of Technology Rourkela-769008, India
[3] Department of Mechanical Engineering, Amity University, Gwalior, MP-474001, India
verma.tikks@gmail.com
tikendra.me@nitmanipur.ac.in

ABSTRACT
In the pressurized/Advanced heavy water reactor (PHWR/AHWR), heavy water is used as both moderator and coolant. In AHWR power unit consist a heater rod bundle which is surrounded by the pressure tube. The cross section consist of water tube is surrounded by the 3 rings of heater rod. These heater rod rings are surrounded by the pressure tube. Pressure tube of power plant allows flowing of the coolant inside the reactor. During loss of coolant in nuclear reactors, temperature of pressure tube rises. Steam available gets condensed at one end of vertical pressure tube. Creation of cold end and hot end invites stresses in pressure tubes. The presence of steam inside the pressurized tube (PT) and high temperature core may fail the pressure tube. The prediction of temperature distribution and the thermal deformation is the prime objective of this project. The main reason of temperature gradient from top to bottom of pressure tube is the laws of the heat transfer.

Keywords: - Pressure tubes, thermal deformation, and deformation.

INTRODUCTION

A nuclear power plant consists of a reactor core where a nuclear chain reaction continuously produces heat. The energy produced in the fuel is removed by the primary heat transport system (PHTS). This heat is utilized to produce steam. The steam drives a turbo-generator to produce electricity. Thermal reactor uses a moderator system to slow down the neutrons produced in the fission reaction to increase the probability of a neutron causing a fission reaction.

The two principal techniques for obtaining numerical solution to boundary value problems are the finite difference method (FDM) and the finite element method (FEM). The FEM was developed for stress analysis. In the area of conduction heat transfer the FDM is still most widely used method. Enery and Carson [1] have compared the FDM and FEM and reportedthat the two methods are comparable for some constant-property steady state solutions but that the FDM is better for most other cases. It is also reported that for FDM is more suitable than FEM for thermal analysis. The FEM generate the temperature distribution results for each node that creates some complication to identify the exact solution at user defined coordinate. Mueller et al. [2] reported prediction of the temperature in a fin cooled by natural convection and radiation. In this paper prediction and measurement of the temperature along a fin cooled by natural convection and radiation are reported. A horizontal fin with a cylindrical cross section heated by conduction along

iJETRM
International Journal of Engineering Technology Research & Management

the fin and dissipated from the surface via natural convection and radiation is analyzed. A simple model was used for radiative heat transfer. A finite difference method used to determine the temperature distribution along the fin. It is seen that the heat loss due to radiation from the fin is 15-20% of the total heat conducted.Mezrhab et al. [3] have presented a numerical study of the radiation-natural convection interactions in a differentially heated cavity with an inner body. A specifically developed numerical model, based on the finite-volume method, is used for the solution of the governing differential-equation. The surface emissivity, the Rayleigh number, and the thermal conductivity ratio were varied parametrically and it is seen that the radiation exchange homogenizes the temperature inside the cavity. The average Nusselt-number increases with increasing surface emissivity, especially at high Rayleigh number.Abdul Aziz et al. [4] has presented and generated homotopy analysis method for heat transfer in a moving fin of variable thermal conductivity which is losing heat simultaneously by convection and radiation to its surroundings. It is seen that the analytic solution is accurate to at least three places of decimal for a wide range of values of the parameters that are commonly encountered in thermal processing application.

W. H. Gray et al. [5] has presented the use of FEM in steady state thermal problem. It is seen that the introduction of a "shape function" and analytically deriving the necessary matrices for each element type, matrix inversion for every element can be eliminated. Wang et al. [6] introduce a paper a finite element code based on the hyperbolic heat conduction equation including the non-Fourier effect in heat conduction. The finite element space discretization is used to obtain a system of differential equations for time. Jiang et al. [7] have presented a study of the effect of filler metal thickness on tensile strength for a stainless steel plate-fin structure by finite element method and experiment. It is seen that the filler metal thickness has a great effect on tensile strength. The tensile strength is increased with the increase of filler metal thickness. Bopche [8] presented an experimental setup and investigate the decay heat removal in advanced nuclear reactors using a single heater rod test facility: Air alone in the annular gap, and identify the temperature distribution on pressure tube by experimental setup.Siddiqa et al. [9] introduce the analysis of magneto hydrodynamic natural convection periodic boundary layer flow of an electrically conducting and optically dense gray viscous fluid along a heated vertical plate. In this study magnetic field is considered in the transverse direction and taken as a sinusoidal function of x. In the analysis radiative heat flux is examined by assuming optically thick radiation limit. The analysis is being made to obtain the solutions valid for liquid metals by taking $Pr << 1$. The results obtained for local skin friction coefficient and local Nusselt number coefficient as well as on the streamlines and isotherm lines are developed graphically.Islamoglu [10] presented the temperature distribution for steady-state heat transfer and the thermal stresses induced by temperature difference in a silicon carbide (SiC) ceramic tube. Finite element method (FEM) was used to compute the temperature and the stress fields. The effect of the axial non-uniform convective heat transfer coefficient on the temperature and thermal stresses have been discussed in terms of the results by FEM. Chu et al. [11] presented the correlation for laminar and turbulent free convection from a horizontal cylinder. The expression for the mean value of nusselt number over the cylinder for all *Ra* and all *Pr* is developed. This expression is applicable for uniform heating as well as for uniform wall temperature and for mass transfer and simultaneous heat and mass transfer. Even simpler expressions are obtained for restricted conditions. These expressions improve upon prior graphical and empirical correlations in both accuracy and convenience.

In the present study, a vertical cylindrical pressure vessel (tube) is considered for mathematical formulation. The thermal source is supplying heat to the vessel from inside

iJETRM
International Journal of Engineering Technology Research & Management

which is transferring in the radically outward direction. The cylindrical annular gaps between the tubes are opened at both the ends, which allow heat transfer to the naturally aspirated air entering from bottom. A temperature distribution is created along the axis because of natural convection. This temperature distribution invites conduction to play a role in the wall of the pressure tube. An experimental facility is fabricated in order to study the heat transfer phenomenon. This physical situation is analogous to the loss of coolant situation of the nuclear reactors. Loss of coolant in the pressure tube increases the temperature of heat source (i.e. nuclear fuel rods) and hence the pressure tube.Also, objective of the present work is to develop a mathematical model using FDM which will have used to predict the surface temperatures of the pressure tube when the source temperature (nuclear fuel temperature) reaches to unsafe values (i.e. 800˚C, 1000˚C, 1200˚C). A finite difference formulation is developed, and a MATLAB computer code is employed. The results predicted using Finite Difference Method have been compared with the Finite element method, experimental results and discussed.

PROBLEM DESCRIPTION

In AHWR power unit consist a heater rod bundle which is surrounded by the pressure tube. The cross section of AHWR unit shown in Fig. 2.1, the water tube is surrounded by the 3 rings of heater rod. The innermost ring having 12 heater rods, middle ring having 18 rods and outermost ring having 24 heater rods. These heater rod rings are surrounded by the pressure tube.

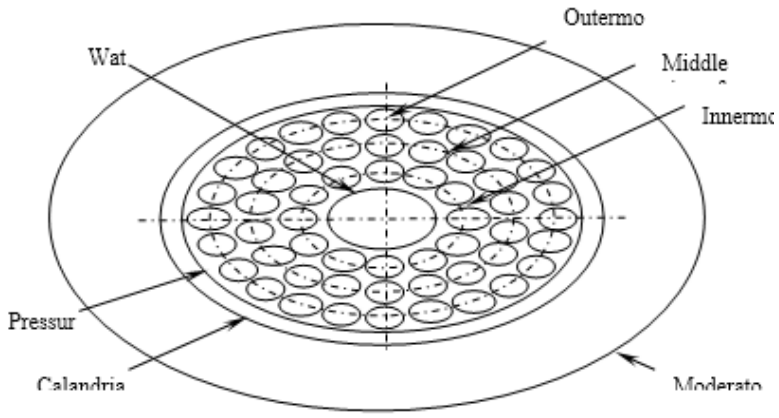

Fig. 2.1 cross section of AHWR

Even after the shutdown of the nuclear chain reaction, decay heat is produced by the radioactive fission products. Long after shut down, considerable amount of decay heat has to be removed from the core. Besides the safe removal of the decay heat, safe shutdown of a nuclear reactor is one of the most important demands for the safety of nuclear power plants. If effective removal of the decay heat is not assured, the decay heat may raise the core temperature to its melting point.

iJETRM
International Journal of Engineering Technology Research & Management

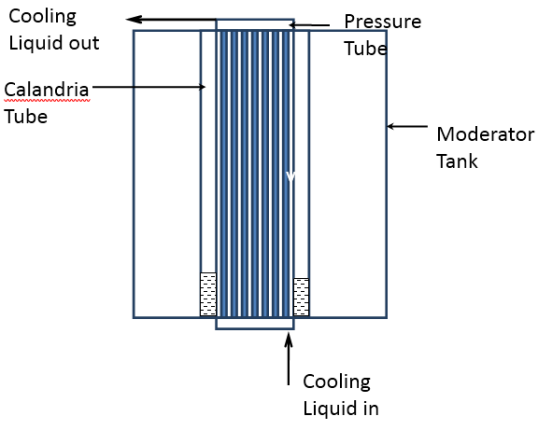

Fig 2.2 Schematic Diagram of Nuclear Power Plant

The presence of steam inside the pressurized tube (PT) as shown in figure 2.2, and high temperature core may fail the pressure tube. The prediction of temperature distribution and the thermal deformation is the prime objective of this work.The main reason of temperature gradient from top to bottom of pressure tube is the laws of the heat transfer.

Experimental Setup

The experimental results have been referred from literature [8] for validation of present FEM results, since it was difficult to fabricate such a facility at our institute.

The schematic of the experimental set up fabricated is as shown in Fig. 3.1. The electrical equipmentis designed for the maximum power supply of 1500 W. The annular space between the pressure tube and calandria tube is specified here as an annular gap. Generally, in the reactor it is filled with an inert gas that isolates the reactor core from the moderator. Electrical power is supplied to the heater rod through two copper bus bars at its ends. Power supply is varied with the help of an autotransformer (10 A). The power supply to the heater is measured with the help of a voltmeter and a clamp-meter is used for monitoring the current.

To detect the surface temperatures of the heater rod, pressure tube and calandria tube, eighteen mineral insulated K-type thermocouples are used. Nine thermocouples are fixed on the outer surface of each component e.g., heater rod and pressure tube. They are brazed at different axial and azimuthal locations. The locations of thermocouples on the surfaces of heater rod, pressure tube are as shown. Thermocouples 1 to 9 are for the heater rod with 1situated near the bottom end and 9near the top end of it, at equal distances. Similarly, 10 to 18 are on the pressure tube outer surface. Temperature data was monitored continuously and recorded with the help of a Data Acquisition System.

iJETRM
International Journal of Engineering Technology Research & Management

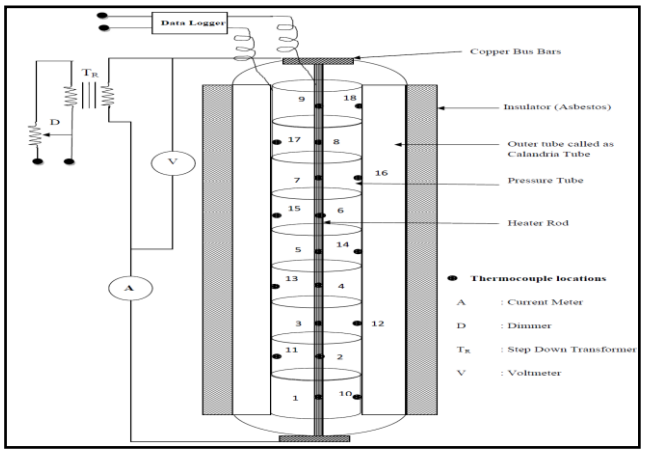

Fig. 3.1 Schematic diagram of single rod set up

1. Governing Equations

Consider a hollow cylinder i.e. pressure tube in nuclear power plants shown in Fig. 3.2. The base is maintaining a constant temperature with the assumption of one directional heat conduction along the tube and steady state heat operation, an energy balance applied to a differential element yields:

$$Q_r + Q_z - Q_{z+dz} - dQ_{loss} = 0$$

Eq. [1]

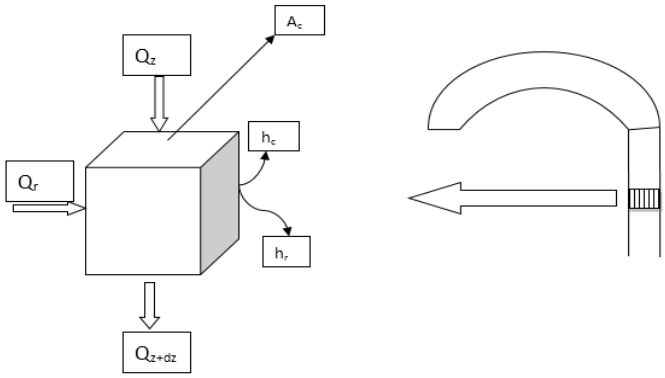

Fig. 3.2 Physical representation of the differential element of the pressure tube

Where, Q_{loss} accounts for heat transfer due to convection and radiation from the surface. With the use of standard equation of conduction convection and radiation the energy balance can be written as:

$$Q_{z+dz} + h_c dA\Delta T + h_r dA\Delta T = Q_r + Q_z$$

Eq. [2]

iJETRM
International Journal of Engineering Technology Research & Management

$$-kA\frac{dt}{dz}-\frac{d}{dz}kA\frac{dt}{dz}+h_c\frac{dA_s(T-T_\infty)}{dz}+\sigma\varepsilon\frac{dA_s(T^4-{T_\infty}^4)}{dz}=\frac{d}{dz}Q_r-kA\frac{dt}{dz}$$

Eq. [3]

$$-\frac{d}{dz}kA\frac{dt}{dz}+h_c\frac{dA_s(T-T_\infty)}{dz}+\sigma\varepsilon\frac{dA_s(T^4-{T_\infty}^4)}{dz}=\frac{d}{dz}Q_r$$

Eq. [4]

In this study, A hollow cylindrical pressure tube with constant cross-section area is considered so that $A_c=\frac{\pi}{4}({D_o}^4-{D_i}^4)$ and $dA_{S_o}=\pi D_o dz$ and $dA_{S_i}=\pi D_i$dz

In theory, $h_c$and k can vary along the length of the fin. In this study, the thermal conductivity k is assumed to be independent of the temperature and thus constant.The convection heat transfer coefficient is assumed to depend on the local surface temperature. The convective heat transfer coefficient, $h_c$is related to the Nusselt number, for which correlation by Churchill and Chu [9] is referred, which is as given in Eq. 5. The correlation is presented below. For the vertical hollow cylinder, the values of radiative heat transfer coefficient (h*r*) are obtained using the experimental analysis [8].

$$Nu_D=\frac{hD}{k_f}=\frac{\left(0.518\times {Ra_D}^{1/4}\right)}{\left[1+(0.559/Pr)^{9/16}\right]^{4/9}}$$

Eq. [5]

$$Ra_D=Gr\times Pr$$

Eq. [6]

Grashof number(Gr) for Vertical wall is given by[17]

$$Gr=\frac{L^3\times g\times\beta\times\Delta T}{\upsilon^2}$$

Eq. [7]

The heat loss term due radiation can be written in a form similar to the convection term with the introduction of the radiation coefficient

$$h_{r_o}\frac{dA_s(T-T_{sur})}{dz}=\sigma\varepsilon\frac{dA_s(T^4-{T_{surr}}^4)}{dz}$$

Eq. [8]

$$h_{r_o}=\epsilon\sigma\left(T^2+{T_{surr}}^2\right)(T+T_{surr})$$

Eq. [9]

Note that, $h_r$depends on the surface temperature, the surrounding temperature, and the fin surface emissivity. In this study, the surroundings are assumed to be completely absorbing, that is black and at the same temperature as the ambient air, that is, $T_{surr.}=T_\infty$.

$$-\frac{d^2T}{dz^2}kA_c=-\frac{dA_{s0}}{dz}(T-T_{\infty o})\left(h_c+h_{r_o}\right)+\frac{dA_{s_i}}{dz}(h_{r_i})(T_{\infty i}-T)$$

Eq. [10]

iJETRM
International Journal of Engineering Technology Research & Management

The convection and radiation loss can be combined into a single term,

$$-\frac{d^2T}{dz^2}kA_c = -\frac{dA_{s0}}{dz}(h)(T - T_{\infty o}) + \frac{dA_{s_i}}{dz}(h_{r_i})(T_{\infty i} - T)$$

Eq. [11]

Where h is the total heat transfer coefficient that accounts for convection and radiation, that is $h = h_c + h_r$

$$kA_c\frac{d^2T}{dz^2} = \frac{h\pi D_o dz(T - T_{\infty o})}{dz} - \frac{h_{r_i}\pi D_i dz(T_{\infty i} - T)}{dz}$$

Eq. [12]

$$\frac{d^2T}{dz^2} = \frac{4hD_o(T - T_{\infty o})}{k({D_o}^2 - {D_i}^2)} - \frac{4h_{r_i}D_i(T_{\infty i} - T)}{k({D_o}^2 - {D_i}^2)}$$

Eq. [13]

Where, $T_{\infty i}$ = Inside Core Temperature (800^{o}c)

$T_{\infty o}$ = Outside Core Temperature (100^{o}c)

h_{r_i} =Inside radiation Heat Transfer Coefficient (25W/m^{2}K)

h= Total Heat Transfer Coefficient (72W/m^{2}K)

D_o = Outside diameter of pressure tube (.038M.)

D_i= Inside Diameter of Pressure Tube (.036M.)

The Finite Difference Equation is referred from text book by Sadikkakac [14], as given below;

$$\frac{dt}{dx}|_{x_m} = \lim_{x\to 0}\frac{T_{(x_m+\Delta x)} - T_{(x_m)}}{\Delta x}$$

Eq. [14]

$$\frac{dt}{dx}|_{x_m} \cong \frac{T_{(x_m+\Delta x)} - T_{(x_m)}}{\Delta x}$$

Eq. [15]

$$\frac{dt}{dx}|_{x_m} = \frac{T_{m+1} - T_m}{\Delta x}$$

Eq. [16]

Eq. [16] is called forward difference form of the first derivative;

$$\frac{dt}{dx}|_{x_m} = \frac{T_m - T_{m-1}}{\Delta x}$$

Eq. [17]

Eq. [17] is known as backward difference form of the first derivative at x_m.Whereas, the "Central difference" form of the first derivative is given in Eq. [18]

$$\frac{dt}{dx}|_{x_m} = \frac{T_{m+1} - T_{m-1}}{2\Delta x}$$

Eq. [18]

Both "Forward and Backward difference" form have a truncation error or discretization error of the order of the magnitude of *'Δx'*. Whereas, the central difference form has a truncation error of the order of the magnitude $(\Delta x)^2$.

The second derivative of T_x, can be approximated in central difference form as:-

iJETRM
International Journal of Engineering Technology Research & Management

$$\frac{d^2T}{dx^2}\Big|_{x_m} = \frac{\left[\left\{\frac{dT}{dx}\right\}_{x_m+\frac{\Delta x}{2}} - \left\{\frac{dT}{dx}\right\}_{x_m-\frac{\Delta x}{2}}\right]}{\Delta x}$$

Eq. [19]

$$\frac{d^2T}{dx^2}\Big|_{x_m} = \frac{\left[\left\{\frac{T_{m+1}-T_m}{\Delta x}\right\}\right] - \left[\left\{\frac{T_m-T_{m-1}}{\Delta x}\right\}\right]}{\Delta x}$$

Eq. [20]

$$\frac{d^2T}{dx^2}\Big|_{x_m} = \frac{T_{m+1}-T_m-T_m+T_{m-1}}{\Delta x^2}$$

Eq. [21]

$$\frac{d^2T}{dx^2}\Big|_{x_m} = \frac{T_{m+1}+T_{m-1}-2T_m}{\Delta x^2}$$

Eq. [22]

Now Using Eq. (9) and Eq. 18

$$\frac{4hD_o(T-T_{\infty o})}{k({D_o}^2-{D_i}^2)} - \frac{4h_{r_i}D_i(T_{\infty i}-T)}{k({D_o}^2-{D_i}^2)} = \frac{T_{m+1}+T_{m-1}-2T_m}{\Delta x^2}$$

Eq. [23]

The tube is divided into 9 elements. Each element is assumed at uniform temperature specified by the center node where thermocouple is fixed. So taking 9 nodes for prediction the temperature distribution of vertical pressure tube, where the values of bottommost and topmost nodes temperatures are input to the mathematical model. The values of radiative heat transfer coefficient values, referred from [8], have been presented in Table 1.

Results and Discussion

The temperature distribution of pressure tube can be evaluated by using ANSYS for different nodes. The prediction of temperature distribution is given below:

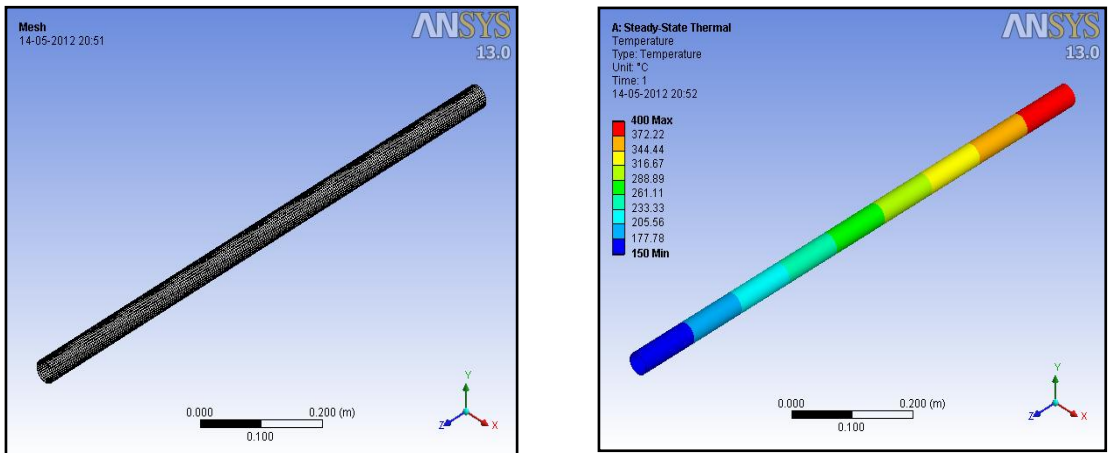

Fig. 5.1Geometry and meshed body of pressure tube

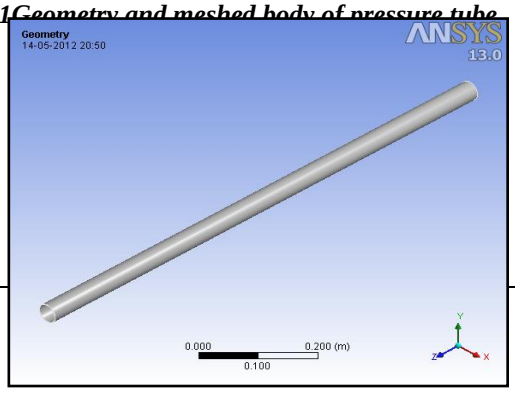

iJETRM
International Journal of Engineering Technology Research & Management

Fig. 5.2 Surface Temperature Distribution of pressure Tube at 400˚C Using ANSYS

It is seen, after analyzing the coordinates of all the nodes, that the temperature of all nodes at a particular elevation is almost same. The arithmetic average of all the temperatures at that particular elevation is taken for pressure tube temperature at the required elevation.The average temperature values and node numbers at that elevation of pressure tube are as shown in Table 5.1.

The comparison among the results obtained using Finite difference method, ANSYS and experimental test runs are as shown in Fig. 5.3. The minimum and maximum percentage deviation for the results obtained using ANSYS software and the experimental results are ±2% and ±18%.

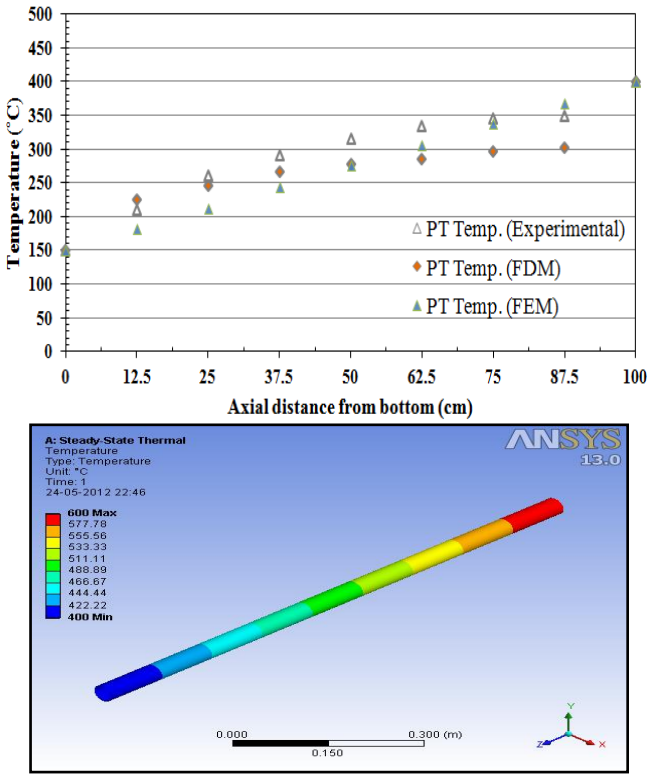

Fig 5.3 Comparison of surface temperatures obtained using FDM, ANSYS and Experimental runs [8] and Contour temperature plot for 600˚C.

The temperature distribution predicted using ANSYS software for maximum pressure tube temperatures of 600˚C, 800˚C and 1100˚C are as shown in Fig. 5.2, 5.3,and 5.6. The slope

iJETRM
International Journal of Engineering Technology Research & Management

of temperature distribution curve is larger in case of 1100˚C, which may create the deformation and stresses in the pressure tube.

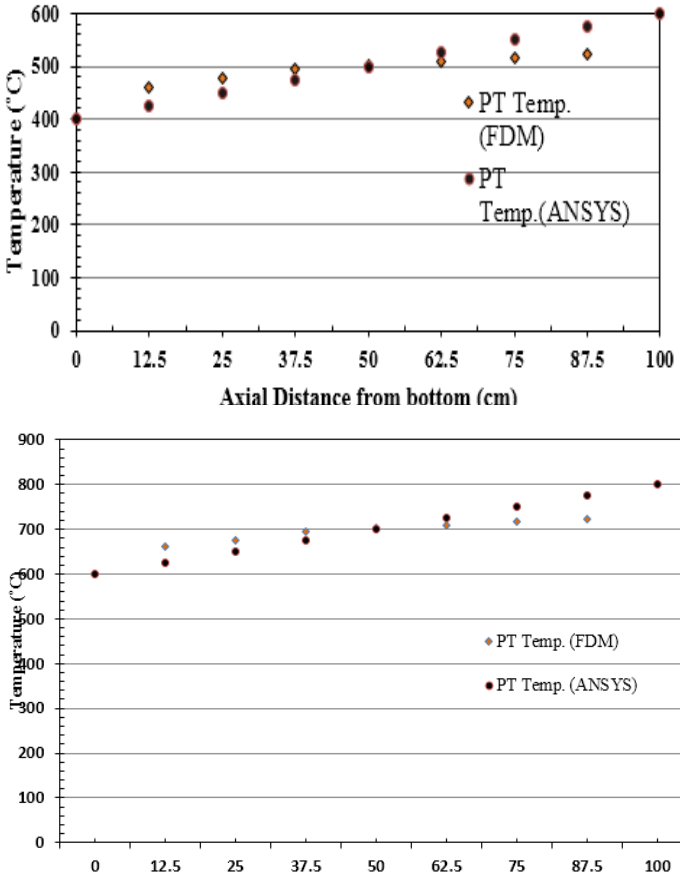

Fig. 5.5 Comparison of Surface Temperature obtained using FDM, ANSYS

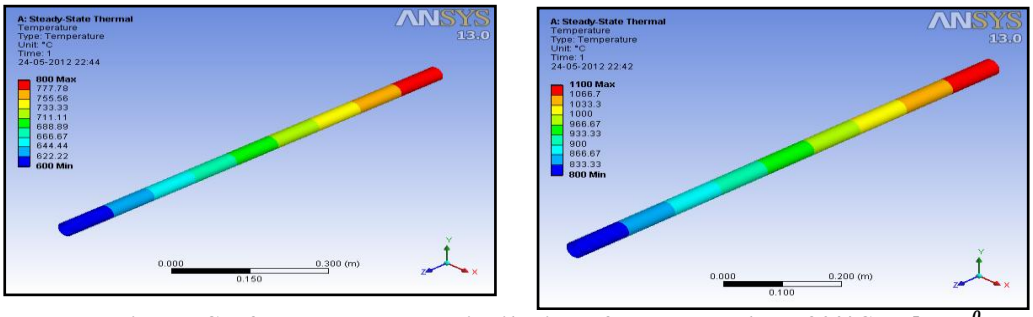

Fig. 5.6 Surface Temperature Distribution of pressure Tube at 800˚C and 100 ^{0}C.

Evaluation of deformation of pressure tube

iJETRM
International Journal of Engineering Technology Research & Management

The above mentioned formulation shows the temperature distribution in pressure tube rod. At the same time thermal stress induced in the pressure tube due to temperature difference.Now the mathematical model for thermal stress and deformation are given below. The stress can be evaluated by formula

$$\sigma = \epsilon \times E$$

Eq.[31]

Where, ϵ, Strain and can be calculated by $\epsilon = \frac{\delta l}{l}$

E, Young's Modulus of Elasticity

Now, the strain is shown by change in length to the original length, but in the problem of pressure tube, the length of pressure tube is fixed from both the ends (Top and Bottom), which create thermal stress in the tube. So there is only possibility of the deformation in radial direction.

The Stress in the pressure tube can be given by

$$\sigma = \frac{D-d}{d} \times E$$

Eq.[32]

Where,

D = Final Diameter

d = Original Diameter

$$d\sigma_t = \frac{D-d}{d} \times E$$

Eq.[33]

The thermal Stress Can be calculated by the formula given below

The final diameter is

$$D = (\alpha \times 10^{-6} dT \times d) + d$$

Eq.[34]

So,

$$d\sigma_t = \frac{(\alpha \times 10^{-6} dT \times d + d) - d}{d} \times E$$

Eq[35]

So the thermal stress for small element is

$$d\sigma_t = (\alpha \times 10^{-6} dT) \times E$$

Eq.[36]

The overall thermal stress can be given by

$$\int_1^2 d\sigma_t = \int_1^2 \alpha \times 10^{-6} \times E \times dT$$

Eq.[37]

or,

iJETRM
International Journal of Engineering Technology Research & Management

$$\sum_{n=1}^{n} d\sigma_t = \sum_{n=1}^{n} \alpha \times 10^{-6} \times E \times dT$$

Eq.[38]

By this mathematical model we can predict the deformation and thermal stress in the pressure tube for various temperatures distribution.The temperature distribution predicted has been done using ANSYS software for maximum pressure tube temperatures of 600˚C, 800˚C and 1100˚C are as shown in Fig. 4.7, 4.10 and 4.12. Now the deformation can be calculated by acquiring same prediction data into static structural for 600˚C, 800˚C and 1100˚C and shown in fig. 5.7 respectively. The contour plot for various temperature are shown in below figure.

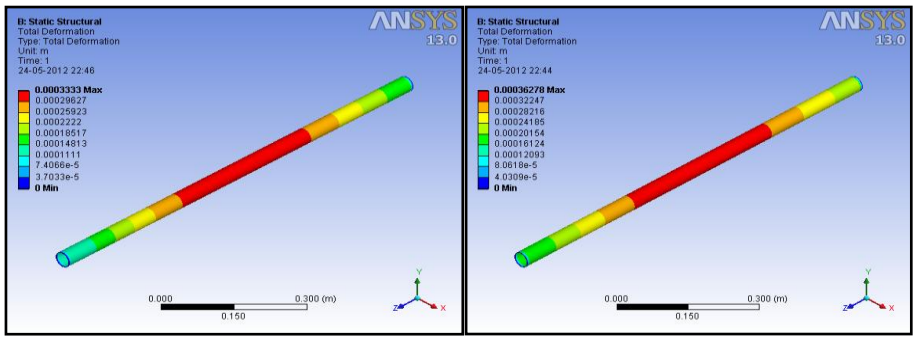

Fig5.7 Deformation of pressure tube for temperature distribution from 400˚C to 600˚C and 800 ˚C

Conclusions

Finite difference method is proved to be an accurate and easy tool for analyzing the actual situations of the nuclear reactor. The percentage deviation created between the experimental results and the predicted values may be due to the assumption made in the analysis and larger uncertainty in choosing values of heat transfer coefficients. The conclusions obtained from the present study are listed as follow.

- The axial temperature distribution is observed in the pressure tube, where temperature is increasing towards the top end. This temperature distribution may be attributed to the natural convection occurring inside and outside the pressure tube. The similar temperature distribution is predicted using FDM and ANSYS analysis.
- The mathematical model developed using FDM can be used to predict surface temperature distribution of pressure tube for higher temperature ranges also, which is experimentally not feasible.
- ANSYS software is also a good tool, to analyze the entire situation, thereby analyzing and generating the solution at radial and azimuthally direction by generating nodes and elements. It's able to evaluate the exact solution at user defined location by refinement and sizing of meshed body, with a good accuracy.
- The surface temperatures could be obtained only at the locations where thermocouples are fixed. ANSYS has been proven a suitable tool for predicting temperatures at all the nodes meshed in the pressure tubing's. It is also seen that almost the same temperatures values have been predicted for one particular elevation which looks fundamentally correct since there is uniformity in boundary conditions of the pressure tube.

iJETRM
International Journal of Engineering Technology Research & Management

REFERENCES

[1] A. F. Emery and W. W. Carson, An evaluation of the use of the finite element method in the computation of temperature, J. Heat Transfer, Trans. A.S.M.E. (1971) 136-145.
[2] D. W. Mueller Jr., H. I. Abu-Mulaweh, Prediction of the temperature in a fin cooled by natural convection and radiation, J. Applied Thermal Engineering 26 (2006) 1662–1668.
[3] A. Mezrhab, H. Bouali , H. Amaoui , M. Bouzidi, Computation of combined natural-convection and radiation heat-transfer in a cavity having a square body at its center, J. Applied Energy 83 (2006) 1004–1023.
[4] Abdul Aziz, F. Khani, Convection–radiation from a continuously moving fin of variable thermal conductivity, Journal of the Franklin Institute 348 (2011) 640–651.
[5] W.H. Gray and N.M. Schnurr, A comparison of the finite element and finite difference methods for the analysis of steady two dimensional heat conduction problems, computer methods in applied mechanics and engineering 6 (1975) 243-245.
[6] B. L. Wang, J. C. Han, Y. G. Sun, A finite element/finite difference scheme for the non-classical heat conduction and associated thermal stresses, Finite Elements in Analysis and Design.
[7] Wenchun Jiang, Jianming Gong, S. T. Tu, A study of the effect of filler metal thickness on tensile strength for a stainless steel plate-fin structure by experiment and finite element method, Materials and Design 31 (2010) 2387–2396.
[8] S. B. Bopche, ArunkumarSridharan, Experimental investigations on decay heat removal in advanced nuclear reactors using a single heater rod test facility: Air alone in the annular gap, Experimental Thermal and Fluid Science 34 (2010) 1456-1474.
[9] Sadia Siddiqa, M.A. Hossain, Rama Subba Reddy Gorla Conduction-radiation effects on periodic magneto hydrodynamic natural convection boundary layer flow along a vertical surface, Int. J. Thermal Sciences 53 (2012) 119-129.
[10]YasarIslamoglu Finite element model for thermal analysis of ceramic heat exchanger tube under axial non-uniform convective heat transfer coefficient, Int. J. Materials and Design 25 (2004) 479–482.
[11]S. W. Churchill, H. H. S. Chu, Correlating equations for laminar and turbulent free convection from a horizontal cylinder, Int. J. Heat Mass Transfer 18 (1975) 1049-1053.
[12]P. Razelos, A critical review of extended surface heat transfer, Heat Transfer Engg. 24 (6) (2003) 11-28.
[13]R. H. Yeh, An analytical study of the optimum dimensions of rectangular fins and cylindrical pin fin, Int. J. Heat Mass Transfer 39 (1996) 1993-2003.
[14]SadikKakac, Heat Conduction, 3rd Edition, Taylor and Francis, (1993), 283-313.
[15] J. N. Reddy, Finite Element Method, 3rd Edition, Tata McGraw Hill, (2005).
[16]P. Sheshu, Textbook of Finite Element Analysis, PHI Learning Pvt. Ltd, (2010).
[17]Dr. D. S. Kumar, Heat and Mass Transfer, Kataria and Sons, (2006-2007).
[18] Release 13.0 Documentation for ANSYS.